Anomalous Gait Feature Classification From 3-D Motion Capture Data

Suil Jeon, Kyoung Min Lee, and Seungbum Koo

***Abstract*—The gait kinematics of an individual is affected by various factors, including age, anthropometry, gender, and disease. Detecting anomalous gait features aids in the diagnosis and treatment of gait-related diseases. The objective of this study was to develop a machine learning method for automatically classifying five anomalous gait features, i.e., toe-out, genu varum, pes planus, hindfoot valgus, and forward head posture features, from three-dimensional data on gait kinematics. Gait data and gait feature labels of 488 subjects were acquired. The orientations of the human body segments during a gait cycle were mapped to a low-dimensional latent gait vector using a variational autoencoder. A two-layer neural network was trained to classify five gait features using logistic regression and calculate an anomalous gait feature vector (AGFV). The proposed network showed balanced accuracies of 82.8% for a toe-out, 85.9% for hindfoot valgus, 80.2% for pes planus, 73.2% for genu varum, and 92.9% for forward head posture when the AGFV was rounded to the nearest zero or 1. Multiple anomalous gait features were detectable using the proposed method, which has a practical advantage over current gait indices, including the gait deviation index with a single value. The overall results confirmed the feasibility of using the proposed method for screening subjects with anomalous gait features using three-dimensional motion capture data.**

***Index Terms*—Human gait, anomalous gait, feedforward neural networks.**

I. Introduction

THE HUMAN gait is one of the fundamental motor skills acquired through repetition. Although gait is a complex motion involving interactions between the environment and multiple segments of the body [1], we can maintain robust and stable locomotion even when experiencing large perturbations [2]. A gait can be affected based on the physical conditions of the human body, including age, anthropometry, gender, disease, leg function, cognitive and affective function, and mental condition [3]. Gait kinematics are highly variable, even in healthy populations. Although an extreme range of joint motion, or an anomalous gait, can exist in healthy individuals, it can also indicate a potential risk of joint disease [4]. The association between gait kinematics and musculoskeletal disorders has been comprehensively investigated [5]–[7].

In a previous study, the dynamic gait index (DGI) was developed to assess the gait, balance, and risk of falling [8]. As a single value, the DGI score is calculated based on eight different gait tests: walking on level surfaces, changing speeds, head-turning in the horizontal and vertical directions, walking and turning 180 degrees before stopping, stepping over and around obstacles, and ascending and descending stairs [8]. Clinical assessments of gait anomalies, which are conducted by clinical experts or physicians, can be affected by their level of expertise or other human factors [9].

Motion capture systems with multiple high-speed cameras have been adopted for a clinical gait assessment. The accuracy and objective measurements of gait kinematics in motion capture systems have been favored for clinical gait assessments [10]–[12]. The gait deviation index (GDI) was proposed to obtain an objective and quantitative measure of gait disorders using 3D motion capture data [13]. The GDI is calculated from the kinematic patterns of the lower limbs, such as the temporal sagittal angle of the knee, the sagittal angle of the ankle, and the phasic progression angle of the foot. To obtain a GDI, the measured lower limb kinematics of a patient were compared with the range of motion of the healthy subjects. Although the measurements from the motion capture system are accurate, the kinematics graphs were again interpreted by a clinician, and a level of expertise can be factored in.

Most clinical gait assessments, including a DGI and a GDI, use manually designed features. Meanwhile, symptoms in a joint can affect the kinematics of multiple joints owing to the nature of gait dynamics [14]. Machine learning methods have been used to provide indices for multiple aspects of an abnormal gait. Previous studies have shown that supervised learning can be used for anomalous gait detection. In the method proposed by Chen et al. [15], a classification network that classifies five abnormal gait kinematics with an accuracy of approximately 88% was implemented using an inertial measurement unit attached to the foot. In addition, a neural network applied to anomalous gait

Manuscript received February 25, 2021; revised June 27, 2021; accepted July 25, 2021. Date of publication August 4, 2021; date of current version February 4, 2022. This work was supported in part by the Basic Science Research Program through the NRF under Grant NRF-2020R1A2C2006057 and in part by the Projects for Research and Development of Police Science and Technology through CRDPST and KNPA under Grant PA-C000001 funded by the Ministry of Science and ICT of the Republic of Korea. *(Corresponding author: Seungbum Koo.)*

Suil Jeon and Seungbum Koo are with the Department of Mechanical Engineering, Korea Advanced Institute of Science and Technology (KAIST), Dajeon 34141, South Korea (e-mail: sjeon1@kaist.ac.kr; skoo@kaist.ac.kr).

Kyoung Min Lee is with the Department of Orthopedic Surgery, Seoul National University Bundang Hospital (SNUH), Seongnam-si 13620, South Korea (e-mail: oasis100@empas.com).

Digital Object Identifier 10.1109/JBHI.2021.3101549

detection was studied by training autoencoders using the 3D kinematics of a normal gait [16]; however, its performance has yet to be tested for practical clinical applications.

In this study, we propose a method for classifying multiple types of anomalous gaits using a machine-learning algorithm and evaluate its classification performance using the gait data of 488 subjects. In addition, a method for extracting an anomalous gait feature vector (AGFV) from high-dimensional gait data with 4848-dimensions is proposed.

Gait data are converted into lower-dimensional vectors through a stack of variational autoencoders (VAEs). The transformed data were then used as inputs into a logistic regression network for AGFV prediction. The logistic regression network predicted the AGFV as continuous values, which could be used to predict the presence of five types of anomalous gait features. The continuous AGFV value can be used as an index of individual anomalous gaits and assist in automated and consistent diagnosis.

II. Related Studies

Many previous studies have utilized gait kinematics to understand gait problems in patients [5]–[7]. The association between gait abnormalities and spatiotemporal gait parameters in patients was investigated. The foot orientation and trajectory of the gait were estimated with temporal detection of the toe-off and heel-strike events from the signals of a shoe-attached IMU sensor [17]. A neural-network-based prediction of the foot clearance parameters in a human gait has been studied to forecast the risk of falling [18]. Spatiotemporal gait parameters such as the walking velocity and step length for 86 subjects with MS were calculated using a pressure sensor, and a statistical analysis was conducted to determine the extent to which each parameter is related to multiple sclerosis [19].

Detection of a freezing of a gait from sensor data in patients with Parkinson's disease has been studied [20]–[24]. Distinct spatiotemporal gait parameter differences were revealed between freezing and non-freezing gaits using wearable sensor data [20]. A quantitative characterization of the freezing of the gait was also conducted. A threshold-based model for predicting the freezing of a gait was proposed under the assumption of a high correlation between the degradation and freezing of the gait [21]. Inertial sensors attached to the lower back and ankles were used to record signals during a gait, and a binary classification of the freezing of a gait was conducted using an autoregressive predictive model and machine learning [22]. A binary classification-based method was investigated for the diagnosis of Parkinson's disease using a machine learning network, including a support vector machine for clinical gait parameters [23]. The freezing of a gait can be classified using a logistic regression classifier from the five gait parameters acquired from the acceleration profile of the ankle obtained using a Bluetooth IMU sensor attached to the ankle [24]. Furthermore, deep neural networks have been used to extract gait features and predict gait scores from 3D body poses obtained from two-dimensional videos in patients with Parkinson's disease [25], [26], [27].

The detection of abnormal gait patterns using sensors such as a pressure sensor and inertial measurement unit built into a shoe insole was also studied [15]. A 3D gyroscope, accelerometer, inertial measurement unit, and bending sensor were used to predict a normal gait and four abnormal gaits, i.e., toe-in, toe-out, over-supination, and heel walking gaits. Using this method, abnormal walking can be classified with an accuracy of approximately 89.9% to 93.38% using a support vector machine.

Currently, gait analyses utilize the three-dimensional kinematics of body segments. Marker-based clinical gait motion capture systems can provide three-dimensional rotations of a full-body human model including the rotation along the segment longitudinal axis [28]; however, the cost of obtaining motion capture data is a bottleneck for collecting a large number of samples [29]. Meanwhile, three-dimensional gait data obtained through a 19-point human stick model are commonly applied for computational human motion studies [16], [30]–[35]. When the positions of the human stick model were sampled at 101 time points of a gait cycle, the 3D gait data had dimensions of $19 \times 3 \times 101 = 5757$. The dimensions of the gait data should be further decreased to train a network for gait feature detection with a limited sample size of the motion capture data.

Many previous studies using a gait analysis extracted only clinical parameters such as joint angles, step length, and cadence [23], [36], [37]. A recent study attempted to classify an anomalous gait from 3D walking data using an autoencoder, which is a machine learning technique. The detection of an anomalous human gait using a sparse deep autoencoder was attempted [16]. The study used only normal walking data for training the autoencoder and assumed that the trained autoencoder would show a poor reconstruction for an anomalous gait. Based on this assumption, a model was proposed for classifying anomalous gaits using the error between the original human gait data and the reconstructed gait data obtained by inputting the data into the autoencoder [16].

III. Methods

A. Data Acquisition

This study was approved by the Institutional Review Board of the Seoul National University Bundang Hospital. Healthy subjects were recruited from the city of Sungnam. The inclusion criteria were no orthopedic disease affecting comfortable walking and between 13 and 75 years in age. The subjects were also screened based on their medical histories. The exclusion criteria were the existence of neuromuscular diseases, history of fracture in the lower limbs, and congenital bone deformities. Diseases unrelated to gait were not included in the criteria. The subjects were tested at the Seoul National University Bundang Hospital. Informed consent was obtained from each subject prior to the test. A total of 500 subjects participated in the study and were tested between 2015 and 2020.

A single operator with 9 years of experience placed photo-reflective skin markers according to the Helen Hayes Marker set [38]. Three-dimensional motion capture data of two gait trials were obtained for each subject using an optical motion capture system (Motion Analysis Co., Santa Rosa, California,

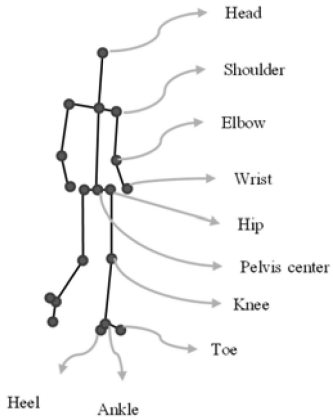

Fig. 1. Nineteen anatomical points including the mid-shoulder and pelvis at the center of the body.

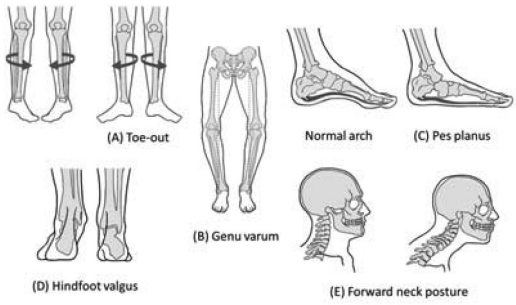

Fig. 2. Illustration of five anomalous gait features (A) toe-out, (B) genu varum, (C) pes planus, (D) hindfoot valgus, and (E) forward head posture.

USA, 100 Hz) with ten cameras. Videos from the front and lateral views were recorded. The subjects walked at a comfortable self-selected speed on a 10-m long flat surface. In the data processing, motion data from 12 subjects were excluded because some of the markers could not be labeled in the motion capture software because of the absence of markers or incomplete trajectories in the motion capture data. Motion data from 488 subjects (248 males, 240 females, average age of 37.1 $\pm$ 16.8 years) were used for this study. Trajectories of the 19 anatomical points shown in Fig. 1 were calculated using motion capture software. Two gait cycles were extracted from each gait trial when the subject walked in the middle of the motion-capture laboratory. Gait data with two gait cycles were split into two one-cycle gait data points. Each gait cycle was from a right heel strike to right heel strike. Thus, four one-cycle gait data were collected from each of the 488 subjects and used in this study.

B. Data Labeling

Five anomalous gait features, that is, toe-out, genu varum, pes planus, hindfoot valgus, and forward head posture (FHP), as illustrated in Fig. 2, were evaluated for all gait data acquired by an orthopedic doctor at Seoul National University Bundang Hospital. The doctor watched the gait videos taken from the front and lateral views of patients to evaluate the presence (1) or absence (0) of each feature. A vector with five binary components was used as the AGFV. The percentages of each anomalous gait feature of the subjects are summarized in Table I.

TABLE I
PREVALENCE OF ANOMALOUS GAIT FEATURES IN THE TESTED SUBJECTS

Feature	Toe-out	Hindfoot valgus	Pes planus	Genu varum	FHP
Percentage	25.4 %	10.4 %	7.2 %	6.4 %	3.9 %
Count	124	51	35	31	19

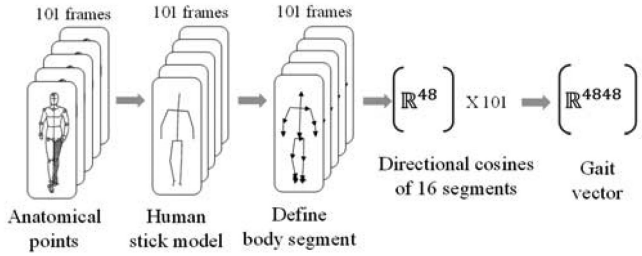

Fig. 3. A gait vector with 4848 components was created from the motion capture data of a gait cycle.

C. Preprocessing

The start position and progression lines of each gait cycle were identified. The three-dimensional position and orientation of each gait cycle were transformed into the origin of the laboratory coordinate system, and the progression line was aligned to the x-axis. The frames of one gait cycle, from a right heel strike to the next right heel strike, were uniformly resampled to obtain 101 frames and normalize the time of a gait cycle. Sixteen body segments were defined by connecting the 19 anatomical points to obtain a stick model representation, as shown in Fig. 3. The orientations of the line segments were represented as direction cosines in the laboratory coordinate system along the progression line of the gait and the z-axis along the vertical group-up direction. Thus, the body configuration can be described as 48 direction cosines. A gait vector with 4848 components can be constructed for a gait cycle with 101 frames.

D. Anomalous Gait Detection Network

The proposed network contains two feed-forward networks to predict the presence of five gait features in a gait cycle, i.e., an encoder network and a classification network, as shown in Fig. 4. The VAE contains encoder and decoder networks [20] and is trained to reconstruct the original input vector. The output of the encoder is a low-dimensional latent vector, which is the means of a multivariate Gaussian distribution. A gait vector with 4848 components was divided into 16 motion vectors for the 16 body segments. Each motion vector contained 303 components. Sixteen VAE networks were trained to reconstruct the motion vectors of the 16 body segments. By dividing a gait vector into 16 motion vectors, we trained the VAE networks using a relatively small number of gait samples. The 16 VAE encoders trained in the 16 VAE networks were used as the encoder network of a one-cycle gait vector, as shown in Fig. 4.

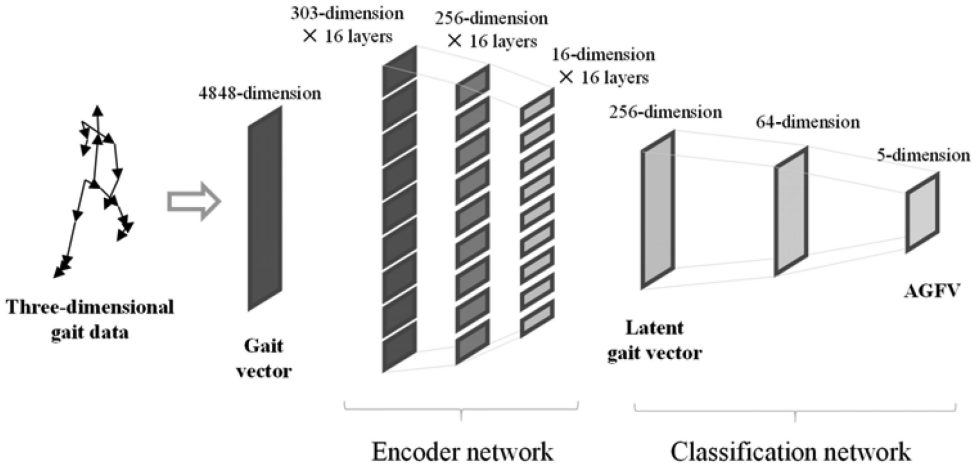

Fig. 4. Anomalous gait detection network.

The latent gait vectors from the encoder network were input into the classification network to predict the presence of five anomalous gait features. The classification network had two hidden layers, 256 × 64 and 64 × 5, as shown in Fig. 4, and a binomial logistic regression was conducted against the labeled anomalous gait features. The ReLU activation function was used in both the encoder and the classification networks. The sigmoid activation function was applied at the end of the classification network to calculate the AGFV. The network was implemented using PyTorch [39]. The loss function of the VAE was represented as a combination of the Kullback–Leibler divergence and the log-likelihood of the training data and the extracted features [40]. All deep learning models were trained using the Adam optimizer with a learning rate of 5e-4 and a maximum of 1e+5 iterations. The running average coefficients for the gradient and its square of the Adam optimizer were set to 0.9 and 0.999, respectively.

Subjects with anomalous gait features accounted for relatively small portions of the data (Table I). The imbalance between the truth and falsity in each feature degraded the prediction accuracy when we used the cross-entropy loss in training the classification network. We used the weighted cross-entropy loss [41], which is defined as follows: Here, γ_k is the weight of the k-th feature used to adjust the imbalance.

$$\mathcal{L}oss = -\sum_{k=1}^{5} \{\gamma_k \cdot p_k(x) \cdot \log(q_k(x)) + (1-\gamma_k) \cdot (1-p_k(x)) \cdot \log(1-q_k(x))\}$$

$$\gamma_k = \frac{\text{number of } negative_k}{number\ of\ positive_k + number\ of\ negative_k}$$

Here, r_k is the ratio of the k-th anomalous gait feature in the training dataset, p_k is the k-th component of the predicted AGFV, and q_k is the k-th component of the actual AGFV, which was labeled by an orthopedic doctor. Gait data from 366 subjects (75%) were used for training, and data from 122 subjects (25%) were used for testing. This training and testing process was repeated to conduct a four-fold cross analysis.

E. Model Evaluation

The performance of the proposed network was compared with that of a previous study that used autoencoders for abnormal gait detection [16]. The study used three autoencoders trained for the x-, y-, and z-coordinates of 17 anatomical positions during a normal gait. The reconstruction error for an abnormal gait was higher than that for a normal gait for the trained autoencoder. The model was used to determine an abnormal gait by comparing the reconstruction errors. The method in [16] was implemented for a direct comparison with the proposed network. Three autoencoders were trained for the x-, y-, and z-coordinates of 17 anatomical positions using the previous method [16]. For each of the five anomalous gait features, the dataset was divided into two groups, with and without the presence of gait features. The 3D anatomical points of all gait datasets were projected onto the X-, Y-, and Z-axes using the proposed method, and their scales were normalized between zero and 1. The Deep Learning Toolbox in MATLAB (MathWorks, Natick, MA, USA) was used to train three autoencoders, the structure of which is defined in [16]. The Kullback–Leibler divergence penalty term and L2-regularization proposed in [16] were applied. The weighted reconstruction error of each gait cycle was calculated using the learned autoencoder, and the gait anomaly was evaluated. Its performance was also calculated through four-fold training and testing.

To adjust for the effect of imbalanced data on the performance measurement, we calculated the balanced accuracy as defined below in addition to the sensitivity and specificity [42], [43]. The balanced accuracy of the imbalanced data matches the precision of the balanced data.

$$\text{Balanced Accuracy} = \frac{1}{2}(Sensitivity + Specificity)$$

In addition, the area under the ROC curve (AUC) was calculated as a general indicator of the performance of the proposed and previous methods [44].

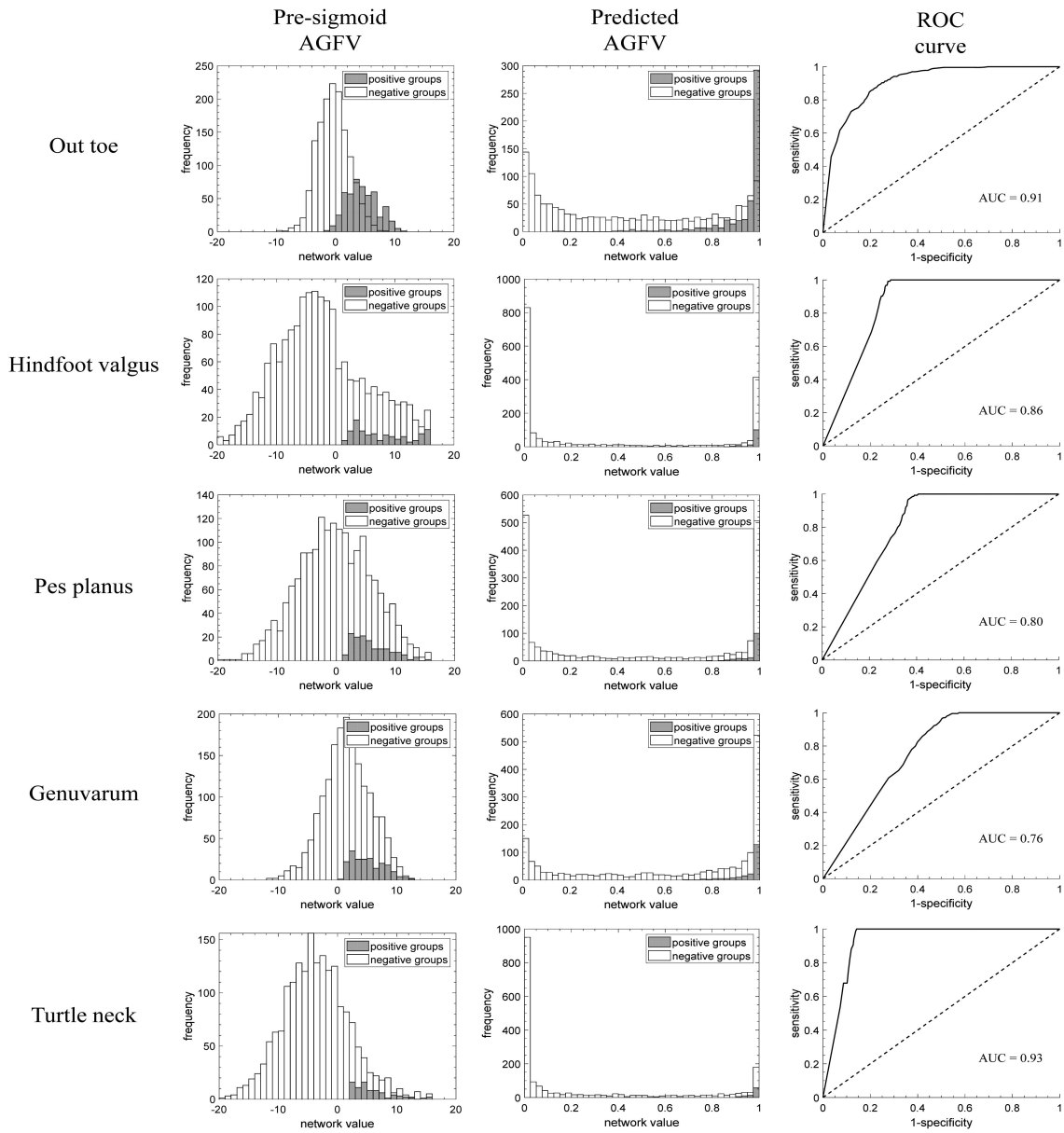

Fig. 5. The AGFV values predicted using the anomalous gait detection network for five gait features (middle). The left column shows the AFGV values before applying the sigmoid function. The receiver operating characteristic curves were calculated depending on the threshold for the AFGV.

IV. Results

The trained network model predicted the AGFV using five components of between zero and 1. The results of the four-fold training and testing of 488 subjects are shown in Fig. 5. The first and second columns show the distribution of the five individual components in the AGFV before and after applying the sigmoid function. Subjects with (positive) and without (negative) anomalous gait features are shown with gray and white bars, respectively.

There were significant overlaps in the AGFV between the positive and negative groups for all five features when the threshold was set to 0.5. Nevertheless, the AGFV for the positive group was predicted to have higher values on average compared to the negative group. For the positive groups (gray bars in the middle column of Fig. 5), the average predicted values were 0.932 for toe-out, 0.985 for hindfoot valgus, 0.974 for pes planus, 0.961 for genu varum, and 0.979 for FHP. For the predictions in the negative groups (white bars in the middle column of Fig. 5), the average values were 0.443 for toe-out, 0.351 for hindfoot valgus, 0.486 for pes planus, 0.640 for genu varum, and 0.257 for FHP.

For individual gait vectors, the sensitivities, specificities, and balanced accuracies of the AGFV features with a threshold value of 0.5, are summarized in Table II. The proposed network had balanced accuracies of 82.8%, 85.9%, 80.2%, 73.2%, and 92.9% for toe-out, hindfoot valgus, pes planus, genu varum, and FHP, respectively. When the same dataset was classified using the previous method [8], the balanced accuracies were found to be approximately 50% for all features.

TABLE II
PREVALENCE OF ANOMALOUS GAIT FEATURES IN THE TESTED SUBJECTS

Classification	Anomalous features	Sensitivity	Specificity	Balanced accuracy	Area under the curve (AUC)
Nguyen et al. (2018)	Out toe	52.9±1.2%	57.5±1.3%	55.2±1.1%	0.55
	Hindfoot valgus	48.9±0.9%	54.0±1.6%	51.5±1.2%	0.49
	Pes planus	57.6±0.8%	52.9±0.7%	55.2±0.8%	0.54
	Genu varum	46.7±1.5%	42.2±1.9%	44.4±1.6%	0.46
	FHP	57.0±0.5%	52.4±1.4%	54.7±0.8%	0.60
Ours	Out toe	88.9±2.7%	76.6±1.2%	82.8±1.8%	0.91
	Hindfoot valgus	99.2±1.5%	72.6±2.9%	85.9±1.2%	0.86
	Pes planus	98.6±1.6%	62.8±3.3%	80.2±1.8%	0.80
	Genu varum	96.6±2.4%	49.8±0.8%	73.2±1.5%	0.76
	FHP	100±0%	86.8±1.6%	92.9±0.8%	0.93

The receiver operating characteristic (ROC) curves were calculated by changing the threshold values, as shown in Fig. 5. To use the proposed network as the first screening process for anomalous gait feature detection, when the sensitivity was set to 95%, the specificities were 67.5% for toe-out, 73.7% for hindfoot valgus, 63.7% for pes planus, 50.5% for genu varum, and 86.2% for FHP. At an equal error rate (where the sensitivity equals the specificity), the balanced accuracy was 80.9% for toe-out, 76.6% for hindfoot valgus, 73.6% for pes planus, 68.6% for genu varum, and 88.1% for FHP.

The performance statistics were also calculated for individual participants. When three or four predictions were true out of the four gait vectors for an individual, the prediction was regarded as true for that person. The balanced accuracies for toe-out, hindfoot valgus, pes planus, genu varum, and FHP were 81.2%, 85.9%, 80.0%, 71.3%, and 92.2%, respectively.

V. DISCUSSION

The proposed network achieved a relatively high accuracy and was shown to be superior to a previous method [16] in detecting the five types of anomalous gait features from a cycle of gait kinematics data. Our method can calculate the presence of five individual clinical gait features related to possible gait diseases [45]. Although the GDI is widely used for a clinical gait assessment [13], it provides only a single number for the gait status. Meanwhile, the proposed method provides scores for five different types of features, which can be further increased if data from a larger cohort are available. An example of using an AGFV is shown in Fig. 6. The AGFVs for six distinct subjects in our dataset were visualized using radar charts. Here, higher values represent the possibility of anomalies in the gait features.

In previous studies, anomalous gait data were acquired by attaching weights to particular body parts of a person without gait abnormalities [16] or by imitating anomalous gait kinematics according to the prescribed protocols [15], [46], [47]. In our study, to reflect the incidence of abnormal gait in the population, a large number of subjects representing the age and gender distributions of the community in Seongnam, South Korea were recruited over a 5-year period. In addition, gait features were labeled by a physician experienced in gait analysis.

The anomalous gait features in our study are highly practical for clinical applications compared with those used in previous studies [9], [15], [46], [47]. Five types of gait features were chosen according to their prevalence within the population [45]. As a potential reason for the lower accuracy of the previous study [16] in application to our dataset, the method in [16] was a semi-supervised learning method [48], [49], and the network was not explicitly trained using positive and negative data, as in the supervised learning.

The body pose during a gait was represented as three direction cosines for each se g ment orientation, assuming a stick figure model. Body segment lengths were not included because they were not features representing abnormal conditions. The rotation along the segment axis could have been included in the gait vectors because we used a marker-based motion capture method, which might increase the classification accuracy while also limiting the application of the suggested method to marker-based motion capture data. The gait vector representation in this study is also applicable to stick figure models obtained from a single camera 3D motion prediction method [50] or marker-less motion capture methods [51].

The acquisition of clinical gait data is extremely expensive [29]. Although we extracted four one-cycle gait data samples from multiple trials of each subject, we acquired only 1952 gait samples. We had to reduce the 4848 dimensions of the original gait vector using dimension-reduction techniques. In this study, to generate a latent gait vector using the VAE, which has been used in previous studies for anomalous feature detection, the number of dimensions of the gait vector was reduced to 256 [41], [52]. The hyperparameters of our VAE and classifier network were adjusted by testing the effect of the number of hidden layers and their sizes [53]. The use of one large VAE incurred a high reconstruction error compared with the separate 16 VAEs

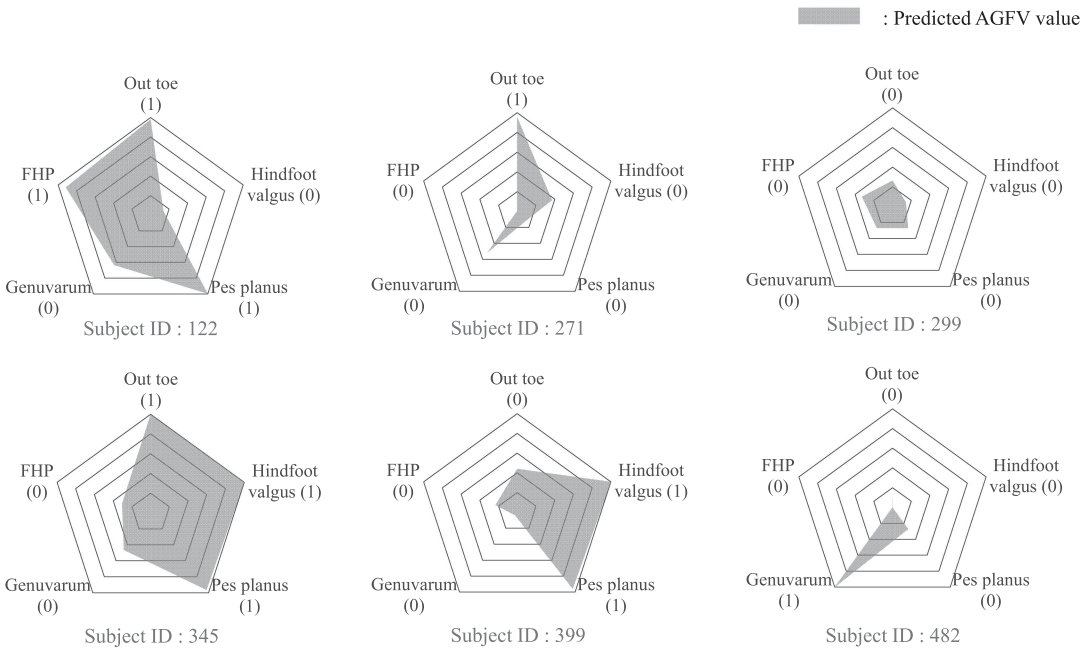

Fig. 6. The radar graphs show the predicted AGFV for five anomalous gait features altogether for six representative subjects. The numbers in the parentheses are the labels done by an orthopaedic doctor. This representation would help understand the state of gait healthiness of patients.

applied in this study. Our study focused on the application of machine methods for clinical applications, and thus a limitation remains in that we did not conduct extensive hyperparameter comparisons. Although the adjacent values of a point in the 4848-dimension gait vector were temporally related, their relationship was not explicitly modeled in our VAE network. Other dimension-reduction methods may generate a more informative latent vector and increase the prediction performance. We did not apply any data augmentation techniques in the present study [54], and if such a suitable method exists, the dimension-reduction network can be removed, and the prediction accuracy can be increased.

VI. Conclusion

Classification networks combined with VAE networks can transform 19-point stick model-based gait data from motion capture systems into latent gait vectors and generate anomalous gait feature vectors with average balanced accuracies of 83.0% for a gait vector and 82.1% for an individual. Although a motion capture system provides accurate temporal joint kinematics, anomalous gait feature detection from clinical gait data has been applied by clinicians. This study showed the possibility of using machine learning algorithms to screen potential gait disorders from clinical motion capture data.

Acknowledgment

The work is based on the Master's thesis of Suil Jeon [50].

References

[1] J. Perry and J. R. Davids, *Gait Analysis: Normal and Pathological Function*, Thorofare, NJ, USA: Slack Inc., 1992.

[2] D. Torricelli, J. Veneman, J. Gonzalez-Vargas, K. Mombaur, and C. D. Remy, "Assessing bipedal locomotion: Towards replicable benchmarks for robotic and robot-assisted locomotion," *Front. Neurorobot.*, vol. 13, 2019, Art. no. 86.

[3] N. B. Alexander, "Gait disorders in older adults," *J. Amer. Geriatr. Soc.*, vol. 44, no. 4, pp. 434–451, 1996.

[4] D. A. Winter, "Biomechanics of normal and pathological gait: Implications for understanding human locomotor control," *J. Motor. Behav.*, vol. 21, no. 4, pp. 337–355, 1989.

[5] L. A. Bolgla, T. R. Malone, B. R. Umberger, and T. L. Uhl, "Hip strength and hip and knee kinematics during stair descent in females with and without patellofemoral pain syndrome," *J. Orthop. Sports Phys. Theory*, vol. 38, no. 1, pp. 12–18, 2008.

[6] Y. F. Shih, C. Y. Chen, W. Y. Chen, and H. C. Lin, "Lower extremity kinematics in children with and without flexible flatfoot: A comparative study," *BMC Musculoskel. Dis.*, vol. 13, no. 1, pp. 1–9, 2012.

[7] K. H. Sung, C. Y. Chung, K. M. Lee, K. B. Kwon, J. H. Lee, and M. S. Park, "Discrepancy between true ankle dorsiflexion and gait kinematics and its association with severity of planovalgus foot deformity," *BMC Musculoskel. Dis.*, vol. 21, pp. 1–8, 2020.

[8] K. C. Chui, M. Jorge, S. C. Yen, and M. M. Lusardi, *Orthotics and Prosthetics in Rehabilitation*, 4th ed., Saunders, Philadelphia, PA, 2019.

[9] S. L. Whitney, A. A. Alghwiri, and A. Alghadir, "An overview of vestibular rehabilitation," *Handbook of Clinical Neurology*, 1st ed. vol. 137, J. M. Furman and T. Lempert, Eds., Amsterdam, The Netherlands; New York, NY, USA: Elsevier, 2016, pp. 187–205.

[10] B. Larsen, M. C. Jacofsky, and D. J. Jacofsky, "Quantitative, comparative assessment of gait between single-radius and multi-radius total knee arthroplasty designs," *J. Arthroplasty*, vol. 30, no. 6, pp. 1062–1067, 2015.

[11] A. Schmitz, M. Ye, G. Boggess, R. Shapiro, R. Yang, and B. Noehren, "The measurement of in vivo joint angles during a squat using a single camera markerless motion capture system as compared to a marker based system," *Gait Posture*, vol. 41, no. 2, pp. 694–698, 2015.

[12] J. Boudarham, N. Roche, D. Pradon, C. Bonnyaud, D. Bensmail, and R. Zory, "Variations in kinematics during clinical gait analysis in stroke patients," *PLoS One*, vol. 8, no. 6, 2013, Art. no. e66421.

[13] M. H. Schwartz and A. Rozumalski, "The Gait Deviation Index: A new comprehensive index of gait pathology," *Gait Posture*, vol. 28, no. 3, pp. 351–357, 2008.

[14] J. L. Astephen, K. J. Deluzio, G. E. Caldwell, and M. J. Dunbar, "Biomechanical changes at the hip, knee, and ankle joints during gait are associated with knee osteoarthritis severity," *J. Orthop. Res.*, vol. 26, no. 3, pp. 332–341, 2008.

[15] M. Chen, B. Huang, and Y. Xu, "Intelligent shoes for abnormal gait detection," in *Proc. IEEE Int. Conf. Robot.*, 2008, pp. 2019–2024.

[16] T. N. Nguyen, H. H. Huynh, and J. Meunier, "Estimating skeleton-based gait abnormality index by sparse deep auto-encoder," in *Proc. IEEE 7th Int. Conf. Consum. Eloctron. (ICCE)* , 2018, pp. 311–315.

[17] B. Mariani, S. Rochat, C. J. Büla, and K. Aminian, "Heel and toe clearance estimation for gait analysis using wireless inertial sensors," *IEEE Trans. Biomed. Eng.*, vol. 59, no. 11, pp. 3162–3168, Nov. 2012.

[18] D. T. Lai, S. B. Taylor, and R. K. Begg, "Prediction of foot clearance parameters as a precursor to forecasting the risk of tripping and falling," *Hum. Movement Sci.*, vol. 31, no. 2, pp. 271–283, 2012.

[19] J. J. Sosnoff, B. M. Sandroff, and R. W. Motl, "Quantifying gait abnormalities in persons with multiple sclerosis with minimal disability," *Gait Posture*, vol. 36, no. 1, pp. 154–156, 2012.

[20] A. Arami, A. Poulakakis-Daktylidis, Y. F. Tai, and E. Burdet, "Prediction of gait freezing in Parkinsonian patients: A binary classification augmented with time series prediction," *IEEE Trans. Neural Syst. Rehabil. Eng.*, vol. 27, no. 9, pp. 1909–1919, Sep. 2019.

[21] L. Palmerini, L. Rocchi, S. Mazilu, E. Gazit, J. M. Hausdorff, and L. Chiari, "Identification of characteristic motor patterns preceding freezing of gait in Parkinson's disease using wearable sensors," *Front. Neurol.*, vol. 8, pp. 394, 2017.

[22] J. C. Schlachetzki *et al.*, "Wearable sensors objectively measure gait parameters in Parkinson's disease," *PLoS One*, vol. 12, no. 10, 2017, Art. no. e0183989.

[23] S. Shetty and Y. S. Rao, "SVM based machine learning approach to identify Parkinson's disease using gait analysis," in *Proc. Int. Conf. Inventive Comput. Technol. (ICICT)*., 2016, pp. 1–5.

[24] K. Polat, "Freezing of gait (FoG) detection using logistic regression in Parkinson's disease from acceleration signals," in *Proc. Sci. Meeting EBBT*., 2019, pp. 1–4.

[25] A. Sabo, S. Mehdizadeh, A. Iaboni, and B. Taati, "Estimating Parkinsonism severity in natural gait videos of older adults with dementia," 2021, *arXiv:2105.03464*.

[26] R. Guo, X. Shao, C. Zhang, and X. Qian, "Multi-scale sparse graph convolutional network for the assessment of Parkinsonian gait," *IEEE Trans. Multimedia*, to be published, doi: 10.1109/TMM.2021.3068609.

[27] M. Lu *et al.*, "Vision-based estimation of mds-updrs gait scores for assessing parkinson's disease motor severity," in *Medical Image Computing and Computer Assisted Intervention MICCAI*, New York, NY, USA: Springer, 2020, pp. 637–647.

[28] A. Muro-De-La-Herran, B. Garcia-Zapirain, and A. Mendez-Zorrilla, "Gait analysis methods: An overview of wearable and non-wearable systems, highlighting clinical applications," *Sensors*, vol. 14, no. 2, pp. 3362–3394, 2014.

[29] D. Hailey and J. A. Tomie, "An assessment of gait analysis in the rehabilitation of children with walking difficulties," *Disabil. Rehabil.*, vol. 22, no. 6, pp. 275–280, 2000.

[30] D. Holden, J. Saito, and T. Komura, "A deep learning framework for character motion synthesis and editing," *ACM Trans. Graphic.*, vol. 35, no. 4, pp. 1–11, 2016.

[31] J. Martinez, M. J. Black, and J. Romero, "On human motion prediction using recurrent neural networks," in *Proc. IEEE Comput. Vis. Pattern Recognit.*, 2017, pp. 2891–2900.

[32] D. C. Luvizon, H. Tabia, and D. Picard, "Learning features combination for human action recognition from skeleton sequences," *Pattern Recognit. Lett.*, vol. 99, pp. 13–20, 2017.

[33] A. Świtoński, A. Polański, and K. Wojciechowski, "Human identification based on the reduced kinematic data of the gait," in *Proc. 7th Int. Symp. Image Signal.*, 2011, pp. 650–655.

[34] D. P. Nguyen, C. B. Phan, and S. Koo, "Predicting body movements for person identification under different walking conditions," *Forensic Sci. Int.*, vol. 290, pp. 303–309, 2018.

[35] M. E. Yumer and N. J. Mitra, "Spectral style transfer for human motion between independent actions," *ACM. Trans. Graphic.*, vol. 35, no. 4, pp. 1–8, 2016.

[36] O. Sofuwa, A. Nieuwboer, K. Desloovere, A. M. Willems, F. Chavret, and I. Jonkers, "Quantitative gait analysis in Parkinson's disease: Comparison with a healthy control group," *Arch. Phys. Med. Rehabil.*, vol. 86, no. 5, pp. 1007–1013, 2005.

[37] O. Blin, A. M. Ferrandez, and G. Serratrice, "Quantitative analysis of gait in Parkinson patients: Increased variability of stride length," *J. Neurol. Sci.*, vol. 98, no. 1, pp. 91–97, 1990.

[38] M. P. Kadaba, H. K. Ramakrishnan, and M. E. Wootten, "Measurement of lower extremity kinematics during level walking," *J. Orthop. Res.*, vol. 8, no. 3, pp. 383–392, 1990.

[39] A. Paszke *et al.*, "PyTorch: An imperative style, high-performance deep learning library," *Adv. Nerual Inf. Process. Syst.*, vol. 32, pp. 8026–8037, 2019.

[40] D. P. Kingma and M. Welling, "Auto-encoding variational Bayes," 2013, *arXiv:1312.6114*.

[41] S. Panchapagesan *et al.*, "Multi-task learning and weighted cross-entropy for DNN-based keyword spotting," in *Proc. Interspeech,* 2016, pp. 760–764.

[42] V. Gulshan *et al.*, "Development and validation of a deep learning algorithm for detection of diabetic retinopathy in retinal fundus photographs," *JAMA*, vol. 316, no. 22, pp. 2402–2410, 2016.

[43] C. Potes, S. Parvaneh, A. Rahman, and B. Conroy, "Ensemble of feature-based and deep learning-based classifiers for detection of abnormal heart sounds," in *Proc. IEEE Comput. Cardiol. Conf.*, 2016, pp. 621–624.

[44] Y. Cong, J. Yuan, and J. Liu, "Sparse reconstruction cost for abnormal event detection," in *Proc. IEEE CVPR*, 2011, pp. 3449–3456.

[45] S. J. Moon *et al.*, "Normative values of physical examinations commonly used for cerebral palsy," *Yonsei Med. J.*, vol. 58, no. 6, pp. 1170–1176, 2017.

[46] S. Potluri, S. Ravuri, C. Diedrich, and L. Schega, "Deep learning based gait abnormality detection using wearable sensor system," in *Proc. 41st Annu. Int. Conf. IEEE Eng. Med. Biol. Soc.*, 2019, pp. 3613–3619.

[47] T. Pandit, H. Nahane, D. Lade, and V. Rao, "Abnormal gait detection by classifying inertial sensor data using transfer learning," in *Proc. 18th IEEE Int. Conf. Mach. Learn. Appl. (ICMLA)*, 2019, pp. 1444–1447.

[48] T. T. Lu, "Fundamental limitations of semi-supervised learning," M.S. thesis, Dept. Math. Comput. Sci., Univ. Waterloo, Waterloo, ON, Canada, 2009.

[49] A. Golovnev, D. Pál, and B. Szorenyi, "The information-theoretic value of unlabeled data in semi-supervised learning," in *Proc. 36th Int. Conf. Mach. Learn. (ICML)*, 2019, pp. 2328–2336.

[50] J. Lee, C. B. Phan, and S. Koo, "Predicting three-dimensional gait parameters with a single camera video sequence," *Int. J. Precis. Eng. Manuf.*, vol. 19, no. 5, vol. pp. 753–759, 2018.

[51] L. Mündermann, S. Corazza, and T. P. Andriacchi, "The evolution of methods for the capture of human movement leading to markerless motion capture for biomechanical applications," *J. Neuroeng. Rehabil.*, vol. 3, no. 1, pp. 1–11, 2006.

[52] D. Park, Y. Hoshi, and C. C. Kemp, "A multimodal anomaly detector for robot-assisted feeding using an LSTM-based variational autoencoder," *IEEE Robot. Autom. Mag. Lett.*, vol. 3, no. 3, pp. 1544–1551, Jul. 2018.

[53] S. Jeon, "Anomalous gait feature detection using three-dimensional walking data with dimension reduction," M.S. thesis, Dept. Mech. Eng., KAIST, Daejeon, Korea, 2021.

[54] L. Perez and J. Wang, "The effectiveness of data augmentation in image classification using deep learning," 2017, *arXiv:1712.04621*.